POTENTIAL OF MULTISPECTRAL IMAGES TAKEN BY SENSORS EMBEDDED IN UAVS FOR MONITORING THE COFFEE CROP IRRIGATION

Vinicius Silva Werneck Orlando [1], George Deroco Martins [2], Eusimio Felisbino Fraga Júnior [2], Aline Barrocá Marra [1], Fernando Vasconcelos Pereira [1], Maria de Lourdes Bueno Trindade Galo [1]

[1] São Paulo State University (UNESP), Presidente Prudente, São Paulo, Brazil - (vinicius.werneck, aline.barroca, fernando.v.pereira, trindade.galo)@unesp.br
[2] Federal University of Uberlândia (UFU), Uberlândia, Minas Gerais, Brazil – (deroco, eusimiofraga)@ufu.br

KEY WORDS: Low-Cost Images, Leaf Water Potential, Agriculture, Coffee Crop, Irrigation, Machine Learning.

ABSTRACT:

Leaf Water Potential (LWP) is an indicator widely used to understand water relations in a coffee tree. Monitoring water potential is a challenge for remote sensing using low-cost multispectral cameras, with images taken by remotely piloted aircraft. The objective of this work was to evaluate the potential of a low-cost camera to discriminate different water treatments in the coffee tree. In addition, the accuracy of models to estimate LWP in the coffee crop was evaluated. The results showed that the NDVI (Normalized Difference Vegetation Index) vegetation index was able to discriminate 61.6 % more plots in a drought regime than the Near-InfraRed (NIR) band in the rainfall regime. For LWP, the architecture that presented the best performance in the detection of water stress was for the first flight (SMOreg algorithm using as predictor variables all bands, Red, Green, and NIR, and the NDVI vegetation index) with RMSE value of 0.1880 and RMSE% of 34.18. For the second flight (Random Tree algorithm, using as predictor variables all bands and NDVI) with RMSE (0.0520) and RMSE% (32.00) values.

1. INTRODUCTION

Agriculture in Brazil is one of the main economic activities due to its large share in the Gross Domestic Product (GDP). The country is the second largest coffee consumer and the largest producer and exporter of cultivated product. In 2020, with the highest production ever recorded, 63.08 million bags of Arabica and Conilon coffee were produced (CONAB, 2022).

The phenological stage of the Arabica coffee tree (*Coffea Arabica L.*) presents a succession of vegetative and reproductive phases, which occur in approximately 2 years. According to Camargo and Camargo (2001), the phenological stage, for tropical conditions in Brazil, was subdivided into six distinct phases, two of which occur in the vegetative period (1st phenological year), and another four in the reproductive period (2nd phenological year). Regarding the first phenological year, the first phase refers to the vegetation and formation of leaf buds, normally from September to March, and the second to the induction and maturation of flower buds (from April to August).

In relation to the second phenological year, the third phase refers to flowering, plumbing and fruit expansion (usually from September to December). The fourth phase is the fruit set, which occurs in midsummer (usually from January to March). At this phase, water stress can be harmful, producing poorly grained fruits. Fruit maturation occurs in the fifth phase, usually between April and June. The sixth and last phase, in July and August, is the senescence of non-primary productive branches, conditioned to the self-pruning of the coffee trees.

Irrigation has been used to correct water deficiencies caused by irregular rainfall, since droughts and temperatures, when unfavourable, are major limitations on coffee production (Damatta and Ramalho, 2006). As irrigation management has the potential to mitigate such negative effects related to coffee cultivation, multiple efforts are being made in several regions of Brazil to improve this process, mainly aimed at the Cerrado region conditions (Vinecky et al., 2017).

In this regard, depending on the phenological stage of the coffee, water stress is a relevant environmental factor as it can be excessively harmful to the growth of the plant (Damatta and Ramalho, 2006). However, when water stress is controlled in the pre-flowering period, it can increase the productivity and nutritional quality of the grain when used rationally (Liu et al., 2018).

An indicator widely used in research aimed at better understanding the water relations of plants is the LWP (Leaf Water Potential) (Ding et al., 2014). LWP is an important agronomic index of the water stress condition of plants, as its decrease can be used as an indicator in the evaluation of physiological processes in plants, such as changes in stomatal behaviour and reduced ability to carry out photosynthesis (Taiz and Zeiger, 2004).

Monitoring water conditions in coffee plantations requires the use of technologies that allow the identification of alterations in plants in relation to those not affected by water stress. According to Damm et al. (2018), Remote Sensing is a powerful technology for agricultural monitoring, allowing the estimation of biophysical parameters that can be used in different areas, such as agrometeorology.

Models generated by Remote Sensing are already being used to detect the first signs of the underdevelopment of coffee under different irrigation management (Silva et al., 2021). Studies show several techniques that can be applied related to LWP, as well as Maciel et al. (2020) who estimated the LWP of coffee areas from the surface reflectance obtained from the Landsat-8 satellite OLI (Operational Land Imager) sensor. The authors indicate that the best model to estimate the LWP was generated using a quadratic

This contribution has been peer-reviewed. The double-blind peer-review was conducted on the basis of the full paper.
https://doi.org/10.5194/isprs-annals-X-1-W1-2023-91-2023 | © Author(s) 2023. CC BY 4.0 License.

NDVI (Normalized Difference Vegetation Index) vegetation index regression (Rouse et al., 1974) ($R^2 > 0.85$ and RMSE < 0.21 Mpa).

Easterday et al. (2019) showed that, using multispectral sensors equipped in unmanned aerial vehicles, it was possible to monitor the progress of a water manipulation experiment in a *Baccharis pilularis* shrub. The authors report that NDVI was the index most capable of distinguishing water treatments, being also more positively correlated with field measurements of LWP.

In a bean culture area, Ranjan et al. (2019) evaluated subplots treated with complete irrigation and half irrigation. From a terrestrial multispectral remote sensing, the authors verified a strong correlation of the NDVI index with the harvest yield (Spearman's correlation coefficient = 0.62, $p < 0.05$) during its growth cycle, thus being an index capable of discriminating the dynamic changes in the water content of the canopy.

In addition, several advanced machine-learning techniques have been developed to adjust empirical models, capable of relating productivity data to factors that influence the crop growth cycle (Bocca and Rodrigues, 2016). In Filgueiras et al. (2019), remote sensing and regression techniques were used to estimate parameters related to water management, such as actual evapotranspiration and soil water content, in commercial corn areas irrigated by pivots. Among the regression models tested, random forests were one of the algorithms that best fit the actual evapotranspiration and the soil water content data. The authors conclude that only with Red and InfraRed wavelengths is it possible to efficiently monitor irrigation.

Considering the importance of monitoring the water conditions of the coffee crop, the objective of this study was to evaluate the potential of low-cost cameras to discriminate different irrigation conditions as well as to estimate LWP through machine learning algorithms.

2. MATERIAL AND METHODS

The experiment was performed in the municipality of Monte Carmelo, Minas Gerais (MG) State, Brazil, which is located in the Mesoregion of Triângulo Mineiro and Alto Paranaíba (Figure 1). The region covers about 1,094 m² of planting of the *Coffea arabica L.* species, Topázio MG cultivar. According to the Köppen-Geiger classification, the climate of the study area is classified as Aw, that is, with hot and rainy summer and cold and dry winter (Alvares et al., 2013).

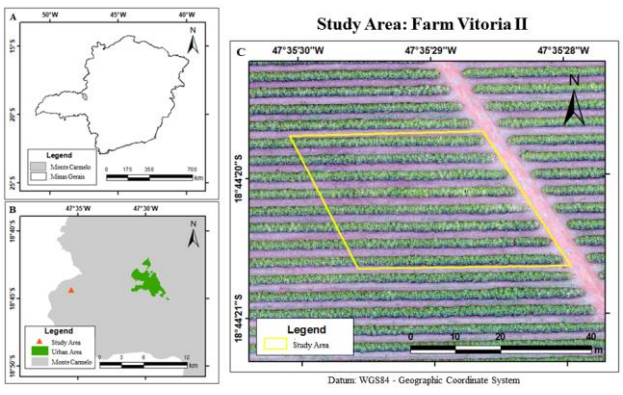

Figure 1. Location of the study area and demarcation of the experimental area highlighted in yellow.

The drip irrigation system is 3.80 x 0.60 m apart. To define the experimental area for this study, a regular sample grid was created with a RBD (Randomized Block Design) with 32 plots. The plots were arranged in eight planting rows submitted to irrigation with two different treatments: normal water and magnetized water and four levels of irrigation depths, 125 %, 100 %, 75 % and 50 %, in which each plot was constituted by a set of 18 plants (Figure 2). Levels of irrigation depths would be water replacement levels. In the 100% treatment, the coffee plants received water replacement to ensure adequate water conditions for the good development of the crop. In the treatments 50 and 75%, the plants received an amount of 50% and 25% less than the ideal water requirement and in the treatment 125%, the plants received 25% of the predicted water volume.

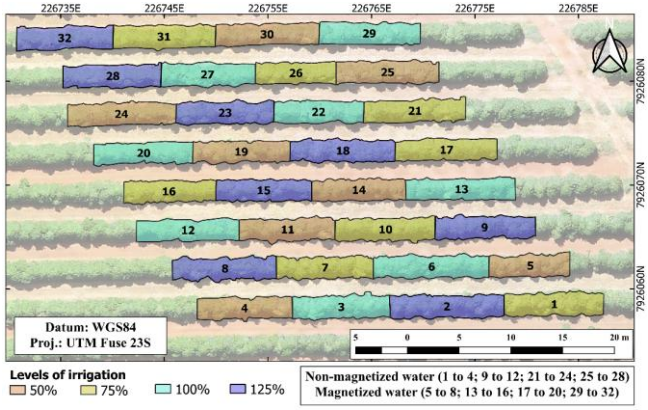

Figure 2. Experiment design for irrigation levels using two water treatments: non-magnetized water (1 to 4; 9 to 12; 21 to 24; 25 to 28) and magnetized water (5 to 8; 13 to 16; 17 to 20; 29 to 32).

2.1 Data Acquisition

Using the fast-static relative positioning method, the plots were delimited by a pair of Promark 500 and Promark 200 GNSS (Global Navigation Satellite System) receivers.

Two aerial surveys were planned to use the DroneDeploy software with a 4 cm GSD (Ground Sample Distance). The aircraft used was the Drone Phantom 4 Advanced with an embedded Mapir Survey 3W Camera operating in the Red, Green and Near-InfraRed (NIR) regions of the electromagnetic spectrum. The characteristics of the Mapir Survey 3W camera are specified in Table 1.

Parameter	Specification
Image resolution	12 Megapixels (4,000 x 3,000 pixels)
Optical lens	87° HFOV (19 mm) f/2.8 Aperture
Red	550 nm center wavelength
Green	660 nm center wavelength
NIR	850 nm center wavelength

Table 1. Mapir Survey 3W sensor specifications.

The first flight was held on October 2, 2018, and the second on March 29, 2019, between 11 am and 12 pm. The radiometric calibration of the images was performed using the Mapir Camera Control software.

The water status of the plants was evaluated *in situ* on the exact two days of the flights, between 5 a.m. and 6 a.m. by the determination of the LWP of the morning, by the Scholander Pressure Chamber. The starting point of line measurements was from bottom to top as shown in Figure 2. Figure 3 illustrates how the samples were selected, collected, and analyzed.

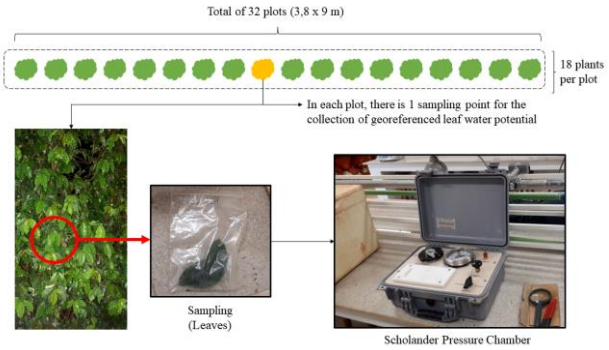

Figure 3. Selection, collection, and analysis of samples, respectively

One plant from each plot was identified and the collection of two leaves (one sample) per plant, totaling 32 sample points. The four levels of irrigation tested were 125 %, 100 %, 75 %, and 50 % required to replenish the coffee tree's water consumption estimated by the daily water balance of the crop (Figure 2). In addition, four repetitions of each treatment were submitted to magnetized water and 4 repetitions of non-magnetized water.

2.2 Evaluation of the sensor potential to discriminate levels of irrigation

Due to the high correlation between the NDVI vegetation index and the NIR spectral range in relation to the coffee crop stress (Martins et al., 2017), a dendrogram analysis was performed to investigate how many irrigation classes would be discriminated from the image generated by the Mapir Survey 3 camera.

The dendrogram was used to analyze clusters of observations as a function of similarity levels. The dendrogram is a diagram that displays the groupings of observations according to the levels of similarity, the number of clusters identified being proportional to the number of classes discriminated. In both cases, the level of similarity used was 3σ (three sigma).

Finally, from the result obtained by the dendrogram, a map showing the discrimination of the irrigation levels was elaborated according to the spectral bands or vegetation index best discriminated of the plots in each aerial survey. Differentiable parcels were represented using a set of colors, while non-differentiable parcels were represented using only one color.

2.3 Adjustment of Machine Learning Models for LWP Prediction

First, the databases were created in the format of tables containing the LWP values collected in the field and the average of the radiometric values extracted from the images of the spectral bands and vegetation index of the region of each evaluated plant.

Two architectural structures for the construction of the prediction model were evaluated. The first subset was composed of the average radiometric values of the NIR band, and the second subset was composed of the average of the radiometric values of the Red, Blue, Green and NIR bands and the NDVI vegetation index.

In total, based on the main algorithms used for estimating agricultural variables from remotely sensed data, highlighted in Damm et al. (2018), three classification algorithms available in the WEKA 3.9.4 (Waikato Environment for Knowledge Analysis) software were trained: Random Tree; Multilayer Perceptron, and SMOreg. In the 32 sampling sites, measurements from 24 sites were used to train the algorithms, and measurements from the remaining 8 sites were used to validate the models.

To validate the quality and determine the best prediction model, the RMSE (Root Mean Square Error) evaluation metric was used, considering as the best estimation model the architecture that presented the lowest RMSE and RMSE% values (Equations 1 and 2).

$$RMSE = \sqrt{\frac{\sum_{i=1}^{n}(x_i - x_{meas})^2}{n}} \quad (1)$$

$$RMSE\ \% = \sqrt{\frac{\sum_{i=1}^{n}(x_i - x_{meas})^2}{n}} X \left(\frac{100Xn}{\sum_{i=1}^{n} x_{meas}}\right) \quad (2)$$

where, x_i represents the estimated LWP value
x_{meas} represents the measured LWP value
n the number of samples

Finally, the images were transformed into a text file with the location and numerical value of each pixel. The model was applied to each of the flights, estimating the LWP in the entire area. Then the text data was rasterized and the maps were generated.

3. RESULTS AND DISCUSSION

3.1 Irrigation level discrimination capability by the images from Mapir Survey 3W Camera

Figure 4 illustrates the grouping of 13 parcels discriminable by NDVI for the first flight. Thus, it would be possible to discriminate 13 of the 32 spectral classes. This result indicates that 40.6 % of the experimental area can be differentiated for the dry condition.

In addition, from the Figure 4 it is possible to infer that the 4th row was the one with the greatest discrimination between classes, being composed by the treatment with magnetized water. As for the first row, there was no discrimination between the plots, which are subjected to non-magnetized water treatment.

Thus, seven plots with magnetized water treatment and five plots with non-magnetized treatment were discriminated. As for water depths, 100% showed greater discrimination in relation to the others, totaling four out of eight discriminable plots. The water depth of 125 % was discriminated in only two of the eight treatments.

This contribution has been peer-reviewed. The double-blind peer-review was conducted on the basis of the full paper.
https://doi.org/10.5194/isprs-annals-X-1-W1-2023-91-2023 | © Author(s) 2023. CC BY 4.0 License.

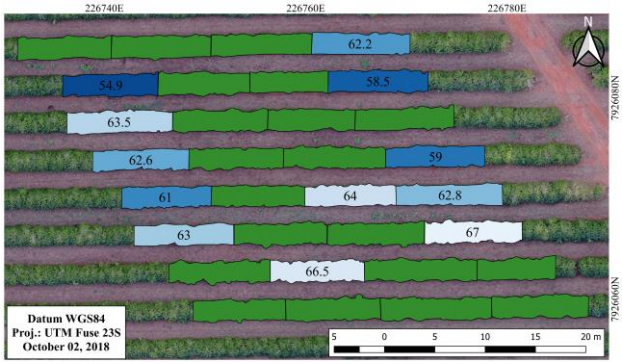

Figure 4. Discrimination of the irrigation levels by NDVI in the first flight generated from the spatialization of the dendrogram. The numbers are the similarity levels of the dendrograms.

For the second flight, Figure 5 shows the dendrogram in the graphical form of a water management class map as a function of the NIR band. Only 15.6% of the plots were differentiated compared to the rainy conditions.

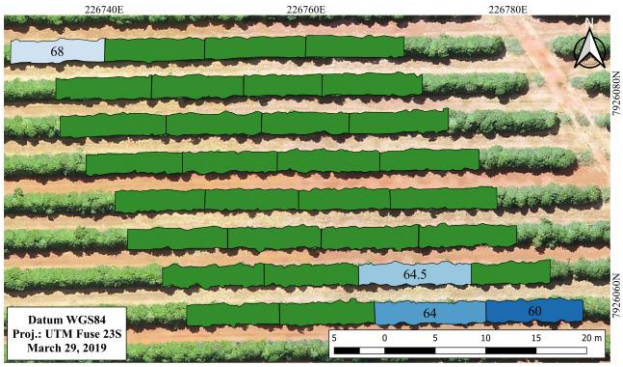

Figure 5. NIR capability for discrimination of the irrigation levels in the second flight generated from the spatialization of the dendrogram. The numbers are the similarity levels of the dendrograms.

From Figure 5, it is possible to notice that the NIR band was able to discriminate only 4 parcels. The discrimination of water treatments was 50 % for each treatment. It is noteworthy that the sensor was not able to discriminate the parcels located from the 3rd to the 7th row. In addition, no water depth of 50 % was discerned. The water depth of 125 % was the most discriminated, being two of the eight treatments.

The results show that none of the plots could be discriminated against simultaneously in the two aerial surveys.

3.2 Empirical Model of the LWP Distribution

Table 2 presents the results obtained for the RMSE and RMSE%, in relation to the first and second flights, for each algorithm and input data set errors.

For the first flight, the SMOreg algorithm showed the best performance to estimate LWP, using as predictor variables all bands and NDVI generated from multispectral images, with the lowest values for RMSE and RMSE% (0.1880 and 34.18, respectively).

Algorithm	Metric	1º flight		2º flight	
		NIR	ALL	NIR	ALL
Multilayer Perceptron	RMSE	0.2305	0.2277	0.0542	0.0587
	RMSE%	41.91	41.40	33.35	36.12
SMOreg	RMSE	0.1932	**0.1880**	0.0563	0.0559
	RMSE%	35.13	**34.18**	34.65	34.40
Random Tree	RMSE	0.3038	0.2552	0.0550	**0.0520**
	RMSE%	55.24	46.40	33.85	**32.00**

Table 2. RMSE and RMSE% results of each algorithm and of both flights.

For the second flight, the Random Tree algorithm presented the best performance to estimate the LWP, using as predictor variables all bands and NDVI generated from multispectral images, presenting the lowest values of RMSE (0.0520) and RMSE% (32.00).

In order to represent the distribution of LWP in the area, the maps illustrated in Figures 6 and 7 were generated by SMOreg and Random Tree, respectively. As shown in Figure 6, the LWP values are homogeneous and are within a relatively high range of data, since they are obtained during the dry season. Thus, the soils expressed values below -0.6 MPa and the canopies showed the highest values, ranging from 0 to -0.59 MPa (Megapascal Pressure Unit).

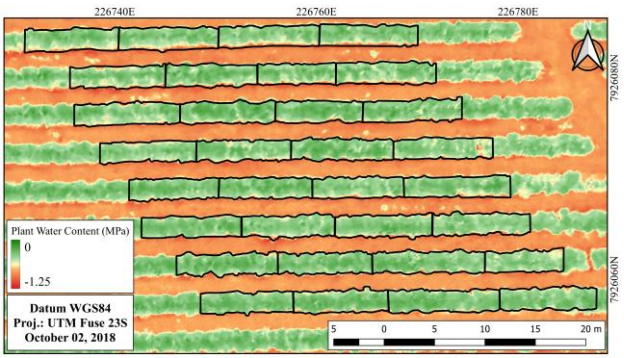

Figure 6. Map of LWP distribution from the image obtained in the first flight.

In early September, producers limit irrigation so that the coffee suffers from induced water stress, aspiring for better flowering and greater uniformity of the types of fruit. Thus, the lowest available water values in the soil are observed due to the induction of water stress by the beginning of the pre-flowering period of the coffee tree.

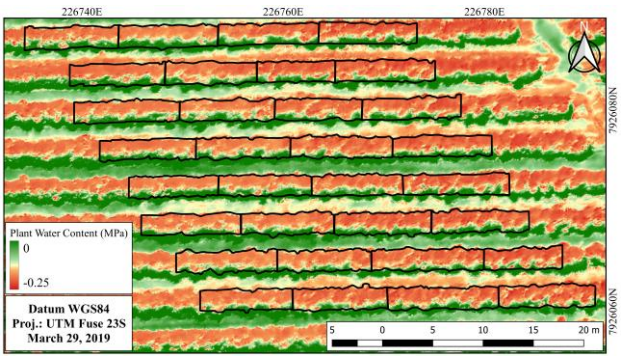

Figure 7. Map of LWP distribution from the image obtained in the second flight.

The second aerial survey, as shown in Figure 7, was carried out at the time of coffee granulation, that is, the phase of grain formation. According to studies carried out by Fraga Júnior et al. (2018), in this same period, water is more accessible to plants, which in turn should have higher values of water potential in the leaf.

The highest LWP class was influenced by soil moisture and, the presence of weeds, competition between the existing inter-rows during the second flight. However, these results are not related to the positions of the water pipes since drip irrigation is not observable between the rows of coffee trees.

4. CONCLUSION

This paper presents a low-cost methodology to estimate coffee LWP from multispectral images and machine learning algorithms, which can be an alternative to classical LWP measurement techniques. However, the algorithms employed in this research produced a high RMSE% while creating models to estimate LWP.

For the definition of water management classes, drought conditions were more favorable to spectral discrimination of experimental plots than rainy conditions. To estimate the LWP, in dry periods the models generated by the SMOreg algorithm were more accurate, while for the rainy period, the most accurate algorithm was the Random Tree.

Due to the high variability observed in the coffee crop, and the effective methodology used in this experiment, it is suggested that the approached techniques can be applied to other areas since this research reflects management and environmental conditions, which can occur in the most diverse areas of planting.

For future works, it is assumed the need to estimate from spectral models, morphological, physiological and phenological parameters of the coffee tree, which, together with the water parameters, may provide information regarding the expected productivity of the crop.

ACKNOWLEDGEMENTS

This work was supported in part by Vitória Farm, AraunahTech and Universidade Federal de Uberlândia. This study was funded in part by the Coordenação de Aperfeiçoamento de Pessoal de Nível Superior – Brasil (CAPES - Grants: nº 88887.817758/2023-00, nº 88887.835305/2023-00, nº 88887.817766/2023-00), and Fundação de Amparo à Pesquisa do Estado de São Paulo (Fapesp - Grant: 2021/06029-7).

REFERENCES

Alvares C.A., Stape, J.L., Sentelhas, P.C., Gonçalves, J.L.M., Sparovek, G., 2013. Köppen's climate classification map for Brazil. *Meteorologische Zeitschrift*. vol. 22w: 711-728.

Bocca, F. F., Rodrigues, L. H. A., 2016. The effect of tuning, feature engineering, and feature selection in data mining applied to rainfed sugarcane yield modelling. *Computers and Electronics in Agriculture*. Vol. 128, Pages 67-76.

Camargo, A. P., Camargo, M. B. P., 2001. Definição e esquematização das fases fenológicas do cafeeiro arábica nas condições tropicais do Brasil. Agrometeorologia. Bragantia, Campinas, 60(1), 65-68.

CONAB. 2022. CONAB: Acompanhamento da safra brasileira, 1º levantamento. https://www.conab.gov.br/info-agro/safras/graos/boletim-da-safra-de-graos (09 January 2022).

Damatta, F.M., Ramalho, J.D.C. 2006. Impacts of drought and temperature stress on coffee physiology and production: A review. *Brazilian Journal of Plant Physiology*, Campinas, v. 18, n. 1. p. 55–81.

Damm, A., Paul-limoges, E., Haghighi, E., Simmer, C. Morsdorf, F., Schneider, D., Van der tole, C., Migliavacca, M., Rascher, U., 2018. Remote sensing of plant-water relations: An overview and future perspectives. *J. Plant Physiol.*, in press.

Ding, Y., Zhang, Y., Zheng, Q., Tyree, M. T., 2014. Pressure–volume curves: revisiting the impact of negative turgor during cell collapse by literature review and simulations of cell micromechanics. *New Phytologist*, Vol.203(2). p.378- 387.

Easterday, K., Kislik, C., Dawson, T.E., Hogan, S., Kelly, M., 2019. Remotely Sensed Water Limitation in Vegetation: Insights from an Experiment with Unmanned Aerial Vehicles (UAVs). Remote Sens. 11, p. 1853.

Filgueiras, R., Almeida, T. S., Mantovani, E. C., Dias, S. H. B., Fernandes-filho, E. I., Cunha, F. F., Venancio, L. P., 2020. Soil water content and actual evapotranspiration predictions using regression algorithms and remote sensing data. Agricultural Water Management, 241, p. 106346.

Fraga Júnior, E. F., Rezende, M. S. de, Fernandes A. L. T., Assis, G. A. de, Rettore Neto, O., Silva Junior, G. J., 2018. Relações hídricas de cafeeiro irrigado sob diferentes lâminas de água eletromagnetizada. In: *Simpósio Brasileiro de pesquisa em cafeicultura irrigada*, XX, Araguari. Anais... Araguari: Fenicafé.

Liu X., Qi Y., Lib F., Yanga Q., Yua L., 2018. Impacts of regulated deficit irrigation on yield, quality and water use efficiency of Arabica coffee under different shading levels in dry and hot regions of southwest China. *Agricultural Water Management*, 204: 292-300.

Maciel, D.A., Silva, V.A., Alves, H.M.R., Volpato, M.M.L., Barbosa, J.P.R.A. D., Souza, V.C.O.D., Santos, M.O., Silveira, H.R.O., Dantas, M.F., Freitas, A.F., Carvalho, G.R., Oliveira dos Santos, J.O., 2020. Leaf water potential of coffee estimated by landsat-8 images. Plos one, 15(3). doi.org/10.1371/journal.pone.0230013

Martins, G. D., Galo, M. de L. B. T., Vieira, B. S., 2017. Detecting and Mapping Root-Knot Nematode Infection in Coffee Crop Using Remote Sensing Measurements. *IEEE Journal of Selected Topics in Applied Earth Observations and Remote Sensing*, p. 1-9.

Ranjan, R., Chandel, A. K., Khot, L.R., Bahlol, H.Y., Zhou, J., Boydston, R.A., Miklas, P.N., 2019. Irrigated Pinto Bean Crop Stress and Yield Assessment using Ground based Low Altitude Remote Sensing Technology. *Inf. Proc. Agric.*

Rouse, J.W.; Haas, R.H.; Schell, J.A.; Deering, D.W., 1974. Monitoring vegetation systems in the great plains with erts. Third ERTS-1 Symposium NASA, NASA SP-351, Washington DC, 309-317.

Silva, P.A.A., Alves, M.C., Sáfadi, T., Pozza, E.A., 2021. Time series analysis of the enhanced vegetation index to detect coffee crop development under different irrigation systems. Journal of Applied Remote Sensing, vol. 15, Issue 1, 014511-014511. doi.org/10.1117/1.JRS.15.014511.

Taiz, L., Zeiger, E. 2004. Fisiologia Vegetal. Universitat Jaume I: Castellón, Spain. 3ed. 720p. ISBN: 9788536302911.

Vinecky, F., Davrieux, F., Mera, A., Alves, G., Lavagnini, G., Leroy, T., Bonnot, F., Rocha, O. C., Bartholo, G. F., Guerra, A. F., Rodrigues, G. C., Marraccini, P., Andrade, A., 2017. Controlled irrigation and nitrogen, phosphorous and potassium fertilization affect the biochemical composition and quality of Arabica coffee beans. *The Journal of Agricultural Science*, 155(6), 902-918. doi.org/10.1017/S0021859616000988.